Restoration of β-adrenergic responsivity in the aging heart

Silvia G. del Villar Ph.D.*, Maartje Westhoff Ph.D.*, Taylor L. Voelker, Eamonn J. Dickson Ph.D., and Rose E. Dixon Ph.D.

** These authors contributed equally to this work.*

Department of Physiology and Membrane Biology, University of California Davis School of Medicine, Davis, CA 95616, USA

Short title: BIN1 decreases functional reserve in old hearts

SGdV: https://orcid.org/0000-0002-5612-4761

MW: https://orcid.org/0000-0002-5421-8609

TLV: https://orcid.org/0000-0002-6779-9350

EJD: https://orcid.org/0000-0001-8619-7630

RED: https://orcid.org/0000-0003-0655-690X

Corresponding author: Rose E. Dixon, redickson@ucdavis.edu Department of Physiology and Membrane Biology, 4112 Tupper Hall, One Shields Avenue, University of California Davis School of Medicine, Davis, CA 95616, USA

Abstract word count: 210

Main text word count (Introduction, Methods, Results, and Discussion): 4977

Abstract

Background: Progressive cardiac hypo-responsivity to *β*-adrenergic receptor (*β*AR)-stimulation occurs with aging, diminishing capacity to manage acute stress, and rendering the heart more vulnerable to systemic stressors including hypertension and diabetes. Disruption of this crucial regulatory mechanism reduces inotropic reserve and lowers the threshold for heart failure. Yet the causal links between aging and *β*-AR hypo-responsivity are unclear.

Methods: Here, using electrophysiology, advanced imaging approaches and biochemistry, we propose a mechanism that explains this age-dependent hypo-responsivity, and a restorative measure to rejuvenate the aging heart.

Results: Our results indicate that cardiac Ca^{2+} channels $Ca_V1.2$ and type 2 ryanodine receptors display altered nanoscale distribution, and impaired *β*AR-stimulated reorganization and recycling with aging that limits their functional augmentation. We find that age-associated overexpression of bridging integrator 1 (BIN1) contributes to dysregulated endosomal recycling and disrupted trafficking dynamics of these channels. BIN1 knockdown restored *β*AR-signaling responsivity and inotropic reserve to youthful levels.

Conclusions: In conclusion, we find that *β*AR hypo-responsivity in the aging heart occurs in part due to expressional upregulation of BIN1 that contributes to deficits in the endosomal pathway, resulting in enlarged endosomes, altered trafficking dynamics of cardiac Ca^{2+} channels, and limiting the plasticity of excitation-contraction coupling. We propose targeted BIN1 knockdown as a novel therapeutic strategy to rejuvenate the aging myocardium.

Keywords:

Calcium channels, ryanodine receptors, aging, $Ca_V1.2$, BIN1, *β*-adrenergic receptors, EC-coupling, clustering

Graphical Abstract

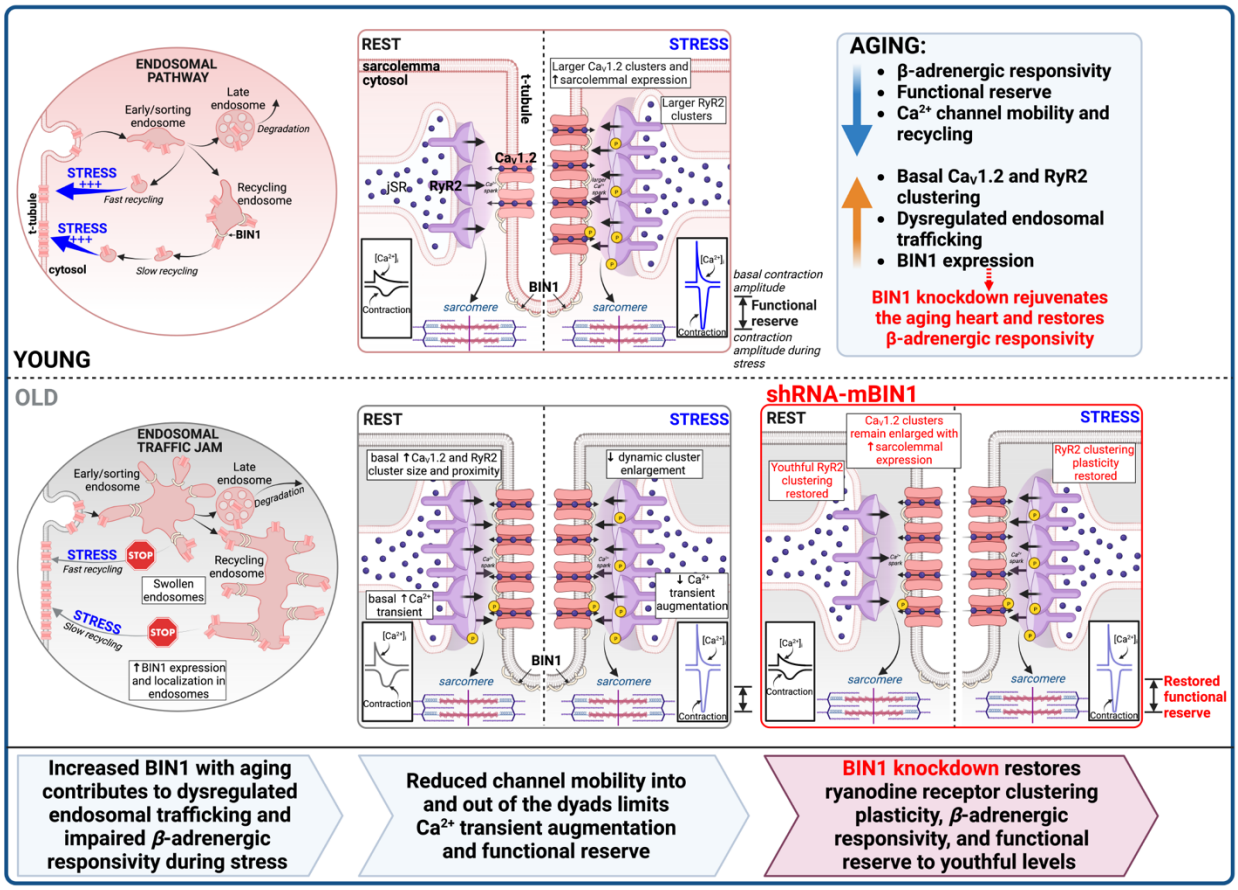

Introduction

Voltage-dependent L-type $Ca_V1.2$ Ca^{2+} channels together with their intracellular cross-dyad partners the type 2 ryanodine receptors (RyR2), orchestrate the Ca^{2+} influx portion of cardiac excitation-contraction (EC) coupling[1, 2]. Functional up-regulation of $Ca_V1.2$ channels via the $G_{\alpha s}$-coupled *β*-adrenergic receptor (*β*-AR) signaling cascade during the fight-or-flight response is an essential element of the normal physiological response to exercise and other acute stressors. Activation of cAMP-dependent protein kinase A (PKA), downstream of *β*-AR stimulation, leads to phosphorylation of the channel complex[3, 4], removing an inhibitory brake and resulting in increased channel open probability (P_o) due to potentiation of longer-duration 'mode 2' openings[5], and an increased number of functional channels[6, 7]. The resultant augmentation in Ca^{2+} influx triggers enhanced release of Ca^{2+} from adjacent sarcoplasmic reticulum (SR)-localized RyR2, producing a positive inotropic response that, along with the chronotropic effects on the pacemaker centers[8], equips the heart to meet acutely enhanced hemodynamic and metabolic demands[3-6]. However, cardiac EC-coupling plasticity is reduced with aging in human[9-12] and animal hearts[13-16], becoming less tunable, and less responsive to *β*-AR-signaling. This precipitates exercise intolerance in the elderly and correlates with increased prevalence of heart failure, as our hearts lose this reactive stimulus and become vulnerable to damage during acutely stressful events when hypoxia and metabolic stress ensue[17, 18].

Weakened myocardial contractile responses to *β*AR-stimulation have been linked to an age-associated decrease in the ability of this signaling cascade to augment intracellular Ca^{2+} transient amplitude[14, 15]. This has been attributed to a reduced capacity to increase $Ca_V1.2$ activity and availability, and thus to diminished Ca^{2+} influx during the action potential (AP)[19]. Recent reports suggest that *β*-AR activation mobilizes a sub-sarcolemmal pool of $Ca_V1.2$ channels, triggering a PKA-dependent, dynamic increase in sarcolemmal $Ca_V1.2$ expression in ventricular myocytes[7, 20]. The consequent enlargement of $Ca_V1.2$ channel clusters facilitates cooperative

channel interactions[20, 21], and amplifies Ca^{2+} influx, revealing a novel mechanism to rapidly tune EC-coupling to meet increased hemodynamic and metabolic demands. We hypothesized that loss of this rheostatic mechanism in aging myocytes could impose a narrow inotropic dynamic range on the system, limiting the response to *β*-AR stimulation.

Nanoscale redistribution and augmentation of cardiac Ca^{2+} channel clustering in response to *β*-AR stimulation also extends to RyR2. Accordingly, acute treatment with the *β*AR-agonist isoproterenol (ISO) or a phosphorylation-inducing cocktail promotes enhanced RyR2 cluster sizes[22, 23], as recently reviewed[24]. This dynamic redistribution of RyR2 into larger clusters is orchestrated by the membrane curvature-forming protein bridging integrator 1 (BIN1)[22] and is linked to increased Ca^{2+} spark frequency which summate to produce larger Ca^{2+} transients[23, 25]. There is widespread agreement that *β*-AR stimulated Ca^{2+} transient augmentation is impaired in the aging myocardium[15, 19], however the underlying mechanisms are not understood.

Here, we present a comprehensive examination of cardiac Ca^{2+} channel function, their nanoscale distribution, and ISO-stimulated redistribution to test the central hypothesis that age-dependent disruption of the on-demand trafficking and clustering of these channels restricts EC-coupling plasticity during myocardial aging and results in *β*-AR hypo-responsivity. We report that old myocytes exhibit basal super-clustering of both $Ca_V1.2$ and RyR2, with no additional dynamic response to ISO. We link these deficits in cardiac Ca^{2+} channel recycling to an age-associated upregulation in BIN1 and the development of endosomal trafficking deficits or “endosomal traffic jams”. Crucially, we find that shRNA-mediated knockdown of BIN1 in old animals restores the young cardiomyocyte phenotype by re-establishing ISO-stimulated RyR2 reorganization, Ca^{2+} transient augmentation, and inotropic reserve.

Methods

A more detailed description of the methods appears in the accompanying supplement.

Ethical Approval

All mouse procedures were approved by the University of California, Davis Institutional Animal Care and Use Committee (IACUC) and were conducted in accordance with National Research Council Guidelines [26].

Myocyte isolation

Old (21-25-month-old) and young (3-5-month-old) ventricular myocytes of both sexes were isolated from C57BL/6J mouse hearts using the retrograde Langendorff perfusion technique as previously described [7, 20].

Electrophysiology

Whole cell electrophysiological signals were recorded using an Axopatch 200B amplifier (Molecular Devices, Sunnyvale, CA, USA).

Line-scan confocal microscopy

Electric field stimulation (E.F.S.) delivered via a Myopacer (IonOptix, LLC., Westwood, MA) or 1 mM caffeine were used to evoke Ca^{2+} transients from fluo-4AM or rhod-2AM (Thermo Scientific, Rockford, IL, USA) loaded myocytes. Transients were recorded on a Zeiss line-scanning LSM 880 confocal (Carl Zeiss Microscopy, LLC., White Plains, NY, USA) and analyzed in ImageJ/FIJI.

TIRF microscopy

TIRF experiments were conducted on live transduced myocytes using an Olympus IX83 inverted microscope as previously described [7].

BIN1 knockdown

To knockdown BIN1 expression in old mice, 5 x 10^{11} vg/ml AAV9-GFP-U6-m-Bin1-shRNA (shRNA-mBIN1) or control AAV9-GFP-scrmb-shRNA (shRNA-scrmb; both from Vector Biolabs, Malvern, PA, USA) were retro-orbitally injected into isoflurane-anesthetized old mice, two weeks before experiments.

Super-resolution imaging

Fixed, immuno-stained cells were imaged on a Leica DMi8 super-resolution microscope or Zeiss LSM 880 with Airyscan detector.

Biochemistry

Specific protein content in whole heart lysates was examined via western blot.

Statistics

N represents the number of animals and *n* represents the number of cells. Data are reported as mean ± SEM. Datasets were compared using paired or unpaired Student's t-tests, one-way ANOVAs, or two-way ANOVAs with Tukey's multiple comparison post-hoc tests as stated in the figure legends. $P < 0.05$ was considered statistically significant.

Data Availability

All datasets generated in the current study are available from the corresponding author upon reasonable request.

Results

β-AR stimulated I_{Ca} augmentation is diminished in aging

Recent evidence suggests that age-dependent changes in cardiac EC-coupling differ between sexes with aged females displaying more preserved contractile function than males[27-30], we thus began with an investigation of the $Ca_V1.2$ channel responses to *β*-AR stimulation by recording whole-cell Ca^{2+} currents (I_{Ca}) from 3-month-old and 24-month-old (henceforth referred to as young and old) male and female ventricular myocytes under control and 100 nM ISO-stimulated conditions. In young male and female myocytes, ISO elicited a 1.60–1.69-fold increase in peak I_{Ca} density (Fig. 1a, b, and Supplemental Table 1). However, old myocytes exhibited a blunted response showing only a 1.18–1.19-fold increase with ISO. In males, basal currents were significantly larger in old myocytes than in young controls (Figs. 1a, and Supplemental Figure Fig. 1a, b, and Table 1), suggestive of enhanced basal PKA-regulation of the channels, potentially leaving less unspent functional reserve to disburse during ISO-stimulation. Examination of the voltage-dependence of conductance supported this hypothesis where a significant leftward-shift was detected relative to young male controls, characteristic of PKA-regulation of cardiac $Ca_V1.2$ channels (Fig. 1c, and Supplemental Figure Fig. 1c and Table 1). Furthermore, current inactivation kinetics were slowed in old male controls relative to young male controls (Supplemental Figure Fig. 1d, e), suggesting a larger proportion of channels were already operating in the longer duration mode 2. On the other hand, despite a trending increase in their basal currents with aging, old female myocytes did not exhibit a significant leftward-shift or slowed inactivation kinetics suggesting that the marginal elevation in basal currents in old female controls are not driven by enhanced PKA-mediated channel complex phosphorylation. The maximal ISO-stimulated current amplitude was similar in young and old myocytes from both sexes (Supplemental Figure Fig. 1a), suggesting that the “ceiling” was intact but that the “floor” or baseline shifts with aging leaving less scope for current augmentation with acute adrenergic stress. We did not observe any change in cell capacitance with aging (Supplemental Figure Fig.

1f). These results suggest that the reduced fold-increase in peak I_{Ca} in old males and females is due to basally increased currents, and that this may underlie the reduced functional reserve and adrenergic hypo-responsivity in aging.

Reduced capacity of β-AR stimulation to tune EC-coupling in old males but not females

Influx of Ca^{2+} through $Ca_V1.2$ channels during action potential mediated depolarization stimulates a larger amplitude Ca^{2+} induced Ca^{2+} release from cross-dyad RyR2 to initiate EC-coupling. The amplitude of the resultant Ca^{2+} transient largely dictates the magnitude of myocardial contraction and the fraction of blood ejected. *β*-AR stimulation enhances both $Ca_V1.2$ and RyR2-mediated Ca^{2+} influx to produce positive inotropy and a greater ejection fraction. We thus examined Ca^{2+} transients in old and young myocytes to investigate the effects of aging on the ability of *β*-AR signaling to tune EC-coupling. Transients evoked from fluo-4AM-loaded myocytes paced at 1 Hz exhibited a 4.1 ± 0.4-fold enhancement in amplitude with ISO in young male cells (Fig. 1d-e, and Supplemental Figure Fig. 1g). Young female myocytes also displayed an amplitude boost with ISO (3.3 ± 0.4-fold) although, in-line with previous reports, this response was less robust than that of males[31, 32]. Aging myocytes from both sexes were able to attain a similar maximal ISO-response amplitude to that seen in their younger counterparts (Supplemental Figure Fig. 1g) but in a parallel with the I_{Ca} results, basal Ca^{2+} transients in aging males were already significantly larger than young males and thus the remaining functional reserve was depleted and the fold-increase with ISO fell to 2.1 ± 0.3 (Fig. 1e). Aging female myocytes displayed no such basal enhancement in Ca^{2+} transient amplitude and exhibited a preserved capacity for amplitude augmentation with ISO (Fig. 1e, and Supplemental Figure Fig. 1g).

Ca^{2+} transient decay rate is an indicator of the effectiveness of Ca^{2+} extrusion mechanisms, mainly SERCA2a, that reinstate Ca^{2+} gradients between beats. PKA-mediated phosphorylation of phospholamban relieves an inhibitory brake on SERCA2a and accelerates

Ca^{2+} extrusion and lusitropy during β-AR stimulation. Accordingly, consistent with the hypothesis that old male myocytes have enhanced basal sympathetic drive, their basal Ca^{2+} transient decay rate was significantly faster than that of young male myocytes and little additional acceleration occurred with ISO in contrast to the significant ISO-induced decay acceleration in young male cells (Fig. 1f). Female myocytes displayed no such age-dependent acceleration in basal Ca^{2+} transient decay rate suggesting they do not exhibit basally enhanced PKA activity, in agreement with the I_{Ca} data. Reflecting the enhanced $Ca_V1.2$ and SERCA activity, rapid application (pico-spritzing) of 20 mM caffeine elicited an ~50% larger Ca^{2+} release from old male myocytes compared to young males or females of either age (Supplemental Figure Fig. 2). Taken together, these data suggest old male myocytes exhibit higher basal PKA-activity presumably downstream of β-AR activation perhaps caused by age-dependent catecholamine spillover and autonomic dysfunction. This results in lower functional reserve in old males and diminishes myocardial responses to acute stress.

Age-dependent alterations in nanoscale distribution and clustering of $Ca_V1.2$ channels

We have previously reported that β-AR activation in young male myocytes stimulates the triggered mobilization of an endosomal pool of pre-formed $Ca_V1.2$ channels into t-tubule, but not crest sarcolemma, facilitating channel clustering and cooperative gating and leading to an amplification of Ca^{2+} influx that contributes to β-AR/cAMP/PKA augmentation of $Ca_V1.2$ currents[7, 20]. To determine whether this ISO-stimulated dynamic channel insertion was still functional in aging myocytes, we examined the nanoscale distribution and clustering of $Ca_V1.2$ in t-tubule and crest regions of young and old myocytes using super-resolution single molecule localization microscopy (SMLM) with and without ISO-stimulation. These experiments confirmed that the super-clustering response to ISO was intact in the t-tubules of young myocytes but absent in old myocytes where the channels were already basally super-clustered (Fig. 2a-b). Indeed, $Ca_V1.2$ channel cluster areas in ISO-treated young myocytes were 28.8% larger on average in male cells, and 31.8 %

larger in female cells when compared to unstimulated controls. However, cluster areas in unstimulated old myocytes of either sex were indistinguishably sized compared to ISO-stimulated young cells and failed to display any significant augmentation in area with ISO (Fig. 2b). This phenomenon was isolated to the t-tubules as crest $Ca_V1.2$ populations showed no significant alteration in any measured parameter (Supplemental Figure Fig. 3). Overall, the age-dependent increase in basal $Ca_V1.2$ channel cluster area and failure to elicit any additional increase with ISO suggests that a larger number of channels are already present in old myocyte t-tubule sarcolemmas and that the ISO-stimulated channel insertion response is impaired in aging myocytes.

Age-dependent alterations in nanoscale distribution and clustering of RyR2 channels

Other groups have reported a similar phosphorylation-induced cluster size expansion of the cross-dyad RyR2s in young ventricular myocytes[22, 23]. In agreement with those reports, SMLM performed on young myocytes immunostained against RyR2, revealed that average RyR2 cluster size grew by 32.7 % in male, and 46.3 % in female myocytes after acute ISO treatment (Fig. 2c and d). However, mean RyR2 cluster areas in unstimulated old myocytes were similarly sized to the expanded clusters observed in ISO-stimulated young myocytes and did not undergo any further expansion with ISO. These findings suggest that the ISO-stimulated nanoscale redistribution of RyR2 is also impaired by aging.

ISO-stimulated enhancement of $Ca_V1.2$-RyR2 interactions is absent in aging

Since functional crosstalk between $Ca_V1.2$ and RyR2 is an essential requirement for cardiac EC-coupling, we next examined the number of sites of proximity between $Ca_V1.2$ and RyR2 using a proximity ligation assay (PLA). In this assay, a fluorescent signal is emitted at each location where $Ca_V1.2$ and RyR2 come within 40 nm of each other[33]. In young myocytes of either sex, acute ISO treatment triggered the emergence of more $Ca_V1.2$-RyR2 proximity sites (Fig. 2e and f). This

phenomenon was not observed in old myocytes, where the number of $Ca_V1.2$-RyR2 proximity sites appeared to have already reached a maximal level in the absence of any exogenous stimulation.

Dynamic TIRF imaging reveals reduced ISO-stimulated $Ca_V1.2$ insertion in aging

The basal super-clustering and absence of a response to ISO in old myocytes may indicate: (i) the endosomal reservoir is empty after already being recycled and inserted; and/or (ii) the trafficking and mobilization of channels is somehow impaired by aging. To interrogate these hypotheses, we visualized real-time dynamics of the channels utilizing a $Ca_V1.2$ "biosensor" approach pioneered by our lab. In this technique adeno-associated virus serotype 9 (AAV9)-$Ca_V\beta_2$-paGFP auxiliary subunits are transduced via retro-orbital injections and then visualized in isolated myocytes using TIRF microscopy as previously described[7, 20]. The relative balance between insertion and endocytosis dictates the overall expression of any membrane protein. An insertion-heavy mismatch between them will lead to increased membrane expression of the protein, while an endocytosis-heavy mismatch will favor reduced expression over time. We used image math to calculate the relative population of channels that were inserted during the ISO treatment, removed/endocytosed, or that remained static during the whole recording. As expected based on our previous studies[7, 20], young myocytes responded to ISO by inserting more $Ca_V1.2$ channels into the sarcolemma than they endocytosed, resulting in a net change in $Ca_V\beta_2$-paGFP in the TIRF footprint that on average amounted to 18% in males and 21.5% in females (Fig. 3a, c-g). However, old myocytes exhibited a comparatively blunted response with fewer ISO-stimulated insertions (Fig. 3c) and a larger population of static channels in the TIRF footprint suggesting impaired mobility (Fig. 3e). Consequently, the ISO-induced change in TIRF footprint $Ca_V\beta_2$-paGFP amounted to only 9.5% in males and 8.4 % in females (Fig. 3g). Female myocytes also exhibited a deficit in channel endocytosis (Fig. 3d). Overall, this experimental series revealed

an age-dependent deficit in ISO-triggered insertion of $Ca_V1.2$, and a shift towards reduced channel mobility or "stranding" at the plasma membrane.

Endosomal traffic jams impede mobilization of endosomal $Ca_V1.2$ reservoirs in aging

We further investigated the effects of aging on the endosomal reservoir and capacity to mobilize $Ca_V1.2$ channel cargo in response to ISO by examining EEA1-positive early endosome, and Rab11-positive recycling endosome pools of $Ca_V1.2$ in young and old myocytes. Accordingly, Airyscan super-resolution imaging on young myocytes revealed immunostained $Ca_V1.2$ cargo on 14-16 % of EEA1 positive pixels in male and female cells (Fig. 4a-b). As we have previously reported, *β*-AR activation stimulates the recycling of a portion of the early endosome $Ca_V1.2$ cargo to the plasma membrane via the Rab4-choreographed fast endosomal recycling pathway[7]. This was evidenced by a significant decrease in the % colocalization between EEA1 and $Ca_V1.2$ after ISO in young males and females with no apparent sexual dimorphism. In old myocytes, there was a trending increase in the percentage of EEA1/$Ca_V1.2$ colocalization in unstimulated cells and no ISO-induced endosomal emptying suggesting trafficking alterations (Fig. 4b). Supporting this idea, EEA1-positive early endosomes were discernibly and quantifiably larger in old myocytes than in young (Fig. 4a and c). Females had a more pronounced change in early endosome size displaying a 37.1% enlargement with age versus the 13.6% enlargement seen in males. Together, these results indicate endosomal traffic jams where an imbalance in cargo trafficking into and out of endosomes leads to their abnormal enlargement[34].

The endosomal traffic jam was observed to extend into the recycling endosomes where a similar age-dependent absence of ISO-induced emptying of their $Ca_V1.2$ cargo was observed in Rab11 and $Ca_V1.2$ double-stained myocytes (Fig. 4d-e). However, recycling endosomes in males underwent a more profound enlargement than females with basal Rab11-positive endosome size trending upward but failing to reach significance (Fig. 4f). Late endosomes did not display any age- or sex-dependent alterations in their size or $Ca_V1.2$ cargo suggesting that the degradation pathway may be intact (Supplemental Figure Fig. 4). Taken together with the dynamic imaging

results in Fig. 3, these data suggest that age-dependent endosomal traffic jams that affect the early and recycling endosomes, impede the trafficking-feedback response to *β-AR* stimulation seen in young mice, and thus alter the dynamic equilibrium of $Ca_V1.2$ channel endocytosis and recycling from the plasma membrane.

BIN1 knockdown in old animals recovers β-AR responsivity and inotropic reserve

BIN1/amphiphysin II has been implicated as playing a role in the development of endosomal traffic jams in Alzheimer's disease-stricken neurons[34]. In the heart, BIN1 is better known for its role in targeted delivery of $Ca_V1.2$[35, 36], t-tubule biogenesis[37], micro-folding[38], and maintenance[39], and in dyad formation[40]. However, in neurons, where there are no t-tubules, BIN1 is known to play a role in mediating endosomal membrane curvature and tubule formation required for cargo exit and recycling from endosomes[41, 42]. BIN1 overexpression has been linked to aging and neurodegeneration in the brain[43-45] and has been seen to produce endosomal expansion and traffic jams[34, 41, 42]. These endosomal pathway issues are thought to contribute to the neuropathogenesis of Alzheimer's disease with endosomal enlargement recognized as the first cytopathological hallmark of the disease[46]. Furthermore, BIN1 expression levels are known to affect ion channel trafficking in both neurons[47] and ventricular myocytes[35, 36]. We thus examined BIN1 expression and localization in young and old myocytes and found an age-associated upregulation and redistribution of BIN1. Old hearts displayed double the BIN1 levels seen in young (Supplemental Figure Fig. 5a-b) and old myocytes exhibited a vesicular, endosomal pattern of BIN1-staining alongside the expected t-tubule population (Supplemental Figure Fig. 5c). Since the BIN1 expression profile was similar in males and females (Supplemental Figure Fig. 5b) we focused our efforts in this experimental series on males. To test whether BIN1 knockdown would restore adrenergic responsivity to aging hearts, we transduced live mice with AAV9-GFP-BIN1-shRNA (shRNA-mBIN1) or AAV9-GFP-scrmb-shRNA (shRNA-scrmb; control) via retro-orbital injection. Two weeks post-injection, hearts were harvested, and western blots confirmed

successful shRNA-mediated knock-down of BIN1 in the old hearts to young heart levels (Fig. 5a-b). Control shRNA-scrmb transduced old hearts had similar BIN1 expression levels to non-transduced old hearts. Surprisingly, and contrary to our hypothesis, whole-cell patch clamp recordings of I_{Ca} in ventricular myocytes isolated from shRNA-mBIN1 transduced hearts did not indicate restoration of ISO responsivity (Fig. 5c-d, and Supplemental Figure Fig. 5d-i). However, Ca^{2+} transient recordings indicated that the inotropic response to ISO had been fully restored to young levels (Fig. 5e-f, and Supplemental Figure Fig. 5j). Notably, Ca^{2+} transient decay kinetics retained the old phenotype, remaining at an accelerated level (Supplemental Figure Fig. 5k) in the transduced cells with and without ISO. This result suggests that SERCA activity and phospholamban phosphorylation remained basally elevated and was not corrected by BIN1 knockdown.

The recovery of Ca^{2+} transient amplitude suggested that BIN1 knockdown may predominantly impact RyR2 function and/or distribution and not $Ca_V1.2$. To investigate that possibility, we performed SMLM on shRNA-mBIN1 transduced myocytes finding the nanoscale distribution of $Ca_V1.2$ was unaltered compared to non-transduced old myocytes in that they remained basally super-clustered and did not recover the super-clustering response to ISO (Fig. 5g-h, and Supplemental Figure Fig. 5l). In contrast, RyR2 appeared rejuvenated and exhibited a young cell-like nanoscale distribution and response to ISO (Fig. 5i-j, and Supplemental Figure Fig. 5m). Overall, these results suggest that knockdown of BIN1 in aging hearts recovers inotropic reserve by restoring RyR2 clustering placticity.

Discussion

This study unveils novel mechanistic insight into why myocardial *β*-AR responsivity is lost as we age. We report four main findings: 1) reduced capacity of *β*-AR stimulation to tune EC-coupling in old males but not females; 2) $Ca_V1.2$ and RyR2 channel clustering, dynamics, and juxta-positioning at dyads are regulated by *β*-AR-mediated signaling, but this regulation is lost during aging; 3) ISO-stimulated Ca^{2+} channel mobility and recycling is impaired in aging due to trafficking deficits; and finally, 4) our results implicate BIN1 overexpression and endosomal traffic jams as causative factors and reveal BIN1 knockdown as a new therapeutic strategy to rejuvenate the aging myocardium's response to *β*-AR signaling, restore functional reserve, and extend cardiovascular health into old age. Our knockdown approach using AAV9 packaged shRNA against BIN1 is rapid, occurring within 2 weeks of retro-orbital injection, and has translational potential as AAVs are approved for use in humans[48].

Prior studies have shown that basal $Ca_V1.2$ activity and *β*-AR-mediated I_{Ca} enhancement are altered with aging[49]. However, the effects on basal $Ca_V1.2$ currents appear to vary depending on sex, species, and possibly even strain with various groups reporting enhanced[49-51], unchanged[52], or reduced[30, 53, 54] currents in aged models. In our hands, myocytes from 24-month-old C57BL/6J mice had enhanced basal $Ca_V1.2$ currents compared to young (3-month-old). While this occurred in both males and females, a sexual dimorphism in the etiology of the basal enhancement appears likely since only males exhibited the hallmark leftward-shift in the voltage-dependence of conductance and slowed inactivation kinetics associated with PKA-modulation of the channel. These findings suggest basal PKA-mediated phosphorylation of $Ca_V1.2$ occurs in aging male myocytes, potentially due to age-associated catecholamine spillover[55]. It is possible that alterations in another post-translational modification of the channel (e.g., S-nitrosylation[32, 56]), exerts a dominant influence that underlies the basal I_{Ca} enhancement in aged females.

Further strengthening the idea of a sexual dimorphism in basal PKA-activity with aging, old male myocytes exhibited more features of PKA-regulation with basally enhanced Ca^{2+} transient amplitudes and accelerated decay kinetics while transients from old females were similar to young. Prior findings on Ca^{2+} transient alterations in the aging myocardium range from basal amplitude augmentation[50, 57] and faster decay kinetics[58] to no or little reported change[54], to basal reduction in CaT amplitude and slower rate of decay[51, 59]. This echoes the variability in age-associated alterations of I_{Ca} and reflects the complexity of aging. Importantly though, and in line with our results, there is agreement that the ability of β-AR-signaling to augment Ca^{2+} transient amplitude and tune EC-coupling and inotropy is diminished with aging[9-16] and that age-associated changes in Ca^{2+} transients and EC-coupling more prominently affect males[28, 30].

This study provides the first evidence linking age-associated β-AR hypo-responsivity to alterations in Ca^{2+} channel clustering and organization. Super-resolution microscopy studies of the nanoscale arrangement of $Ca_V1.2$ and RyR2 have fueled the emerging concept that tunable insertion, recycling, and clustering of these channels physiologically during receptor signaling cascades or pathologically in disease, affects Ca^{2+} release efficiency and myocardial contractility[7, 20, 23, 24, 60-62]. Larger $Ca_V1.2$ clusters facilitate enhanced $Ca_V1.2$-$Ca_V1.2$ physical interactions and cooperative gating that amplifies I_{Ca}[20, 21, 63] while larger RyR2 clusters favor enhanced Ca^{2+} spark frequency[25] and larger Ca^{2+} transients. We previously reported that acute β-AR activation in young ventricular myocytes promotes rapid, dynamic augmentation of sarcolemmal $Ca_V1.2$ channel abundance as channels are mobilized from pre-made endosomal reservoirs via fast and slow recycling pathways[7, 20]. Here, super-resolution microscopy and dynamic channel tracking experiments demonstrated that this response is impaired with aging in males and females where $Ca_V1.2$ are already super-clustered to a similar extent to that seen in young ISO-stimulated myocytes. These results correlated with the basally elevated I_{Ca} and impaired current augmentation with ISO seen in our patch-clamp experiments, hinting that the functional reserve of $Ca_V1.2$ cargo in the endosomal reservoir has already been expended and/or endosomal

recycling pathways are impaired. Our data suggest the latter is true, revealing reduced ISO-induced insertions in old myocytes, an aggregation of channels on swollen endosomes, and a larger pool of static channels that appear stranded in the sarcolemma. Whether this larger pool of static channels reflects increased lifetime of $Ca_V1.2$ in the membrane remains to be established though females show an additional impairment in endocytosis that would support that. The main conclusion from this data is that the endosomal pathway and homeostatic regulation of $Ca_V1.2$ channel expression at the sarcolemma is impaired with aging and this is further borne out in our examination of the endosomal populations where $Ca_V1.2$ mobilization from early and recycling endosomes is impaired in old myocytes.

On the other side of the dyadic cleft, a similar picture emerges for RyR2 which also display enlarged basal clusters that fail to undergo augmentation with ISO in aging myocytes. Other groups have reported phosphorylation-stimulated clustering of RyR2[22, 23] but this is the first report of disruption of this dynamic response with aging. Furthermore, it is the first to find that spatial proximity between $Ca_V1.2$ and RyR2 increases with acute ISO in young myocytes. This suggests rapid dynamic formation or expansion of dyads during ISO-stimulation.

The implication here is that β-AR activation stimulates parallel $Ca_V1.2$ and RyR2 cluster expansion on either side of the dyadic cleft to maximize the efficiency of Ca^{2+} release but that this additional tuning capacity or reserve is lost with aging and is apparently already expended at rest. Old females and males both exhibit this parallel basal super-clustering, yet only males have basally enhanced Ca^{2+} transients. This appears paradoxical but one must consider that SR Ca^{2+} release during EC-coupling is dictated not just by the proximity of $Ca_V1.2$ and RyR2 and the number of dyads but also by SR Ca^{2+} content[64].

We find old males have a larger SR Ca^{2+} load and a trending increase in fractional release while old females have no such age-associated change and a tendency toward reduced fractional release compared to young. Accordingly, our data suggests this sexual dimorphism in basal Ca^{2+} transient amplitude at least partially reflects differences in basal SR Ca^{2+} load. However, load

differences are unlikely to be the full story as one would predict that the combination of enhanced $Ca_V1.2$ and RyR2 clustering and proximity, and larger basal I_{Ca} should stimulate enhanced CICR and larger Ca^{2+} transients. Sex and age-dependent alterations in SR Ca^{2+} buffering and/or differences in RyR2 post-translational modification and sensitivity may further constrain female EC-coupling gain but these remain to be investigated.

Cardiac RyR2 trafficking and mobility is poorly understood and understudied but one report has linked RyR2 redistribution upon phosphorylation to BIN1, evidenced by reduced recruitment of phosphorylated RyR2 to dyadic regions in cardiac-specific *BIN1* knockout cardiomyocytes[22]. Our data indicates that BIN1 overexpression with aging affects RyR2 clustering and positioning at the dyad.

In the heart, the role of BIN1 in endosome-size regulation or recycling has not been explored until now. Our data shows that endosomal enlargement occurs in aging ventricular myocytes, indicating deficiencies in the endosomal pathway. Examination of endosomal $Ca_V1.2$ pools revealed impaired ability to mobilize and recycle endosomal cargo in aging myocytes from males and females, restricting their ISO-stimulated recycling and insertion. It was somewhat surprising however, to find that BIN1 knockdown in old mice had a more profound effect on RyR2 distribution, Ca^{2+} transient amplitude, and inotropy than it does on $Ca_V1.2$. RyR2 nanoscale distribution was rejuvenated by BIN1 knockdown in old hearts but $Ca_V1.2$ still exhibited the old super-clustered phenotype and heightened basal I_{Ca}. It is possible that another yet unidentified regulator(s) of $Ca_V1.2$ is altered with aging and has a stabilizing effect on sarcolemmal expression.

Isoforms of BIN1 containing a clathrin and adaptor protein-2 binding motif (CLAP) support the membrane curvature and tubulation of endosomal membranes that must occur to control exit of cargo from these organelles through the slow recycling pathway[42, 65, 66]. *BIN1* contains up to 20 exons and alternative splicing leads to the generation of at least 12 different isoforms[67]. In young mouse hearts, a unique cardiac splice variant is present along with at least three others, only two of which contain at least one exon (13) of the CLAP motif (encoded by exons 13-16)[38].

It is unknown whether this single exon is enough to regulate endosomal size and recycling or whether additional splice variants are expressed in the aging heart.

While we focus on the post-synaptic effector side of the cardiac sympathetic nervous system, it is noteworthy that there are also age-associated changes on the presynaptic side. There, despite an age-associated degeneration of sympathetic nerve fibers[58], overall sympathetic nerve firing-frequency increases with aging[68]. This, coupled with reduced norepinephrine reuptake into the neurons leads to catecholamine spillover to the plasma[55]. Chronic activation of *β*-ARs by the enhanced plasma norepinephrine concentration is linked to their desensitization and various groups have found reduced densities of *β*-ARs[14] or altered cAMP generation[69-71] in the aging heart that likely contribute to the reduced responsivity to *β*-AR activation with aging. Crucially, here we find that knockdown of BIN1 can rescue cardiac responsivity to *β*-AR stimulation and that these effects can be traced to effects on RyR2 distribution. However, BIN1 is also expressed in neurons and thus AAV9-mediated BIN1 knockdown may also affect sympathetic nerve fibers, and this could conceivably play a part in the rescue phenomenon. This idea should be explored in future studies.

In summary, we find that BIN1 knockdown restores Ca^{2+} transient augmentation in response to *β*AR-stimulation in the aging myocardium. Since Ca^{2+} transient amplitude is the major determinant of myocardial contractility, the positive inotropic response is thus recovered. This study sets the groundwork for future work and raises the hope that a similar approach could restore exercise tolerance and capacity to endure acute stress in elderly patients.

Acknowledgments

We extend our thanks to Drs. James Trimmer and Nicholas Vierra for generously providing their in-house generated affinity purified rabbit polyclonal antibody Cav1.2 II-III (RRID:AB_2922674). We thank Dr. L. Fernando Santana and Heather Spooner for reading and providing critical suggestions on our manuscript. The Graphical Abstract was generated using Biorender.com.

Sources of Funding

This work was supported by NIH National Institute on Aging Grant R01AG063796 to R.E.D.; National Institute of General Medical Sciences (NIGMS) Grant R01GM127513 to E.J.D.; and by the NIGMS funded Pharmacology Training Program (T32GM099608) and later by an AHA Predoctoral Fellowship (827909), both to T.L.V.

Disclosures

None.

References

1. Bers DM. Cardiac excitation-contraction coupling. *Nature*. 2002;415:198-205.

2. Westhoff M and Dixon RE. Mechanisms and Regulation of Cardiac $Ca_V1.2$ Trafficking. *Int J Mol Sci*. 2021;22.

3. Osterrieder W, Brum G, Hescheler J, Trautwein W, Flockerzi V and Hofmann F. Injection of subunits of cyclic AMP-dependent protein kinase into cardiac myocytes modulates Ca^{2+} current. *Nature*. 1982;298:576-8.

4. Hartzell HC, Mery PF, Fischmeister R and Szabo G. Sympathetic regulation of cardiac calcium current is due exclusively to cAMP-dependent phosphorylation. *Nature*. 1991;351:573-6.

5. Yue DT, Herzig S and Marban E. β-adrenergic stimulation of calcium channels occurs by potentiation of high-activity gating modes. *Proc Natl Acad Sci U S A*. 1990;87:753-7.

6. Bean BP, Nowycky MC and Tsien RW. β-adrenergic modulation of calcium channels in frog ventricular heart cells. *Nature*. 1984;307:371-5.

7. Del Villar SG, Voelker TL, Westhoff M, Reddy GR, Spooner HC, Navedo MF, Dickson EJ and Dixon RE. β-Adrenergic control of sarcolemmal $Ca_V1.2$ abundance by small GTPase Rab proteins. *Proc Natl Acad Sci U S A*. 2021;118.

8. Choi S, Vivas O, Baudot M and Moreno CM. Aging Alters the Formation and Functionality of Signaling Microdomains Between L-type Calcium Channels and β_2-Adrenergic Receptors in Cardiac Pacemaker Cells. *Front Physiol*. 2022;13:805909.

9. White M, Roden R, Minobe W, Khan MF, Larrabee P, Wollmering M, Port JD, Anderson F, Campbell D, Feldman AM and et al. Age-related changes in beta-adrenergic neuroeffector systems in the human heart. *Circulation*. 1994;90:1225-38.

10. Lakatta EG. Deficient Neuroendocrine Regulation of the Cardiovascular-System with Advancing Age in Healthy Humans. *Circulation*. 1993;87:631-636.

11. Stratton JR, Cerqueira MD, Schwartz RS, Levy WC, Veith RC, Kahn SE and Abrass IB. Differences in cardiovascular responses to isoproterenol in relation to age and exercise training in healthy men. *Circulation*. 1992;86:504-12.

12. Davies CH, Ferrara N and Harding SE. Beta-adrenoceptor function changes with age of subject in myocytes from non-failing human ventricle. *Cardiovascular research*. 1996;31:152-6.

13. Lakatta EG, Gerstenblith G, Angell CS, Shock NW and Weisfeldt ML. Diminished inotropic response of aged myocardium to catecholamines. *Circ Res*. 1975;36:262-9.

14. Xiao RP, Tomhave ED, Wang DJ, Ji X, Boluyt MO, Cheng H, Lakatta EG and Koch WJ. Age-associated reductions in cardiac β_1- and β_2-adrenergic responses without changes in inhibitory G proteins or receptor kinases. *J Clin Invest*. 1998;101:1273-82.

15. Xiao RP, Spurgeon HA, O'Connor F and Lakatta EG. Age-associated changes in β-adrenergic modulation on rat cardiac excitation-contraction coupling. *J Clin Invest*. 1994;94:2051-9.

16. Cerbai E, Guerra L, Varani K, Barbieri M, Borea PA and Mugelli A. β-adrenoceptor subtypes in young and old rat ventricular myocytes: a combined patch-clamp and binding study. *Br J Pharmacol*. 1995;116:1835-42.

17. Strait JB and Lakatta EG. Aging-Associated Cardiovascular Changes and Their Relationship to Heart Failure. *Heart Failure Clinics*. 2012;8:143-164.

18. Ferrara N, Komici K, Corbi G, Pagano G, Furgi G, Rengo C, Femminella GD, Leosco D and Bonaduce D. β-adrenergic receptor responsiveness in aging heart and clinical implications. *Front Physiol*. 2014;4:396.

19. Lakatta EG and Sollott SJ. Perspectives on mammalian cardiovascular aging: humans to molecules. *Comp Biochem Physiol A Mol Integr Physiol*. 2002;132:699-721.

20. Ito DW, Hannigan KI, Ghosh D, Xu B, Del Villar SG, Xiang YK, Dickson EJ, Navedo MF and Dixon RE. β-adrenergic-mediated dynamic augmentation of sarcolemmal $Ca_V1.2$ clustering and co-operativity in ventricular myocytes. *J Physiol*. 2019;597:2139-2162.

21. Dixon RE, Navedo MF, Binder MD and Santana LF. Mechanisms and Physiological Implications of Cooperative Gating of Ion Channels Clusters. *Physiological reviews*. 2021.

22. Fu Y, Shaw SA, Naami R, Vuong CL, Basheer WA, Guo X and Hong T. Isoproterenol Promotes Rapid Ryanodine Receptor Movement to Bridging Integrator 1 (BIN1)-Organized Dyads. *Circulation*. 2016;133:388-97.

23. Asghari P, Scriven DR, Ng M, Panwar P, Chou KC, van Petegem F and Moore ED. Cardiac ryanodine receptor distribution is dynamic and changed by auxiliary proteins and post-translational modification. *Elife*. 2020;9.

24. Dixon RE. Nanoscale Organization, Regulation, and Dynamic Reorganization of Cardiac Calcium Channels. *Front Physiol*. 2021;12:810408.

25. Galice S, Xie Y, Yang Y, Sato D and Bers DM. Size Matters: Ryanodine Receptor Cluster Size Affects Arrhythmogenic Sarcoplasmic Reticulum Calcium Release. *J Am Heart Assoc*. 2018;7.

26. National Research Council (U.S.). Committee for the Update of the Guide for the Care and Use of Laboratory Animals., Institute for Laboratory Animal Research (U.S.) and National Academies Press (U.S.). *Guide for the care and use of laboratory animals.* 8th ed. Washington, D.C.: National Academies Press; 2011.

27. Feridooni HA, Dibb KM and Howlett SE. How cardiomyocyte excitation, calcium release and contraction become altered with age. *J Mol Cell Cardiol*. 2015;83:62-72.

28. Howlett SE. Age-associated changes in excitation-contraction coupling are more prominent in ventricular myocytes from male rats than in myocytes from female rats. *Am J Physiol Heart Circ Physiol*. 2010;298:H659-70.

29. Fares E and Howlett SE. Effect of age on cardiac excitation-contraction coupling. *Clin Exp Pharmacol Physiol*. 2010;37:1-7.

30. Grandy SA and Howlett SE. Cardiac excitation-contraction coupling is altered in myocytes from aged male mice but not in cells from aged female mice. *Am J Physiol Heart Circ Physiol*. 2006;291:H2362-70.

31. Vizgirda VM, Wahler GM, Sondgeroth KL, Ziolo MT and Schwertz DW. Mechanisms of sex differences in rat cardiac myocyte response to beta-adrenergic stimulation. *Am J Physiol Heart Circ Physiol*. 2002;282:H256-63.

32. Sun J, Picht E, Ginsburg KS, Bers DM, Steenbergen C and Murphy E. Hypercontractile female hearts exhibit increased S-nitrosylation of the L-type Ca^{2+} channel α_1 subunit and reduced ischemia/reperfusion injury. *Circ Res*. 2006;98:403-11.

33. Fredriksson S, Gullberg M, Jarvius J, Olsson C, Pietras K, Gustafsdottir SM, Ostman A and Landegren U. Protein detection using proximity-dependent DNA ligation assays. *Nature biotechnology*. 2002;20:473-7.

34. Small SA, Simoes-Spassov S, Mayeux R and Petsko GA. Endosomal Traffic Jams Represent a Pathogenic Hub and Therapeutic Target in Alzheimer's Disease. *Trends Neurosci*. 2017;40:592-602.

35. Hong TT, Smyth JW, Gao D, Chu KY, Vogan JM, Fong TS, Jensen BC, Colecraft HM and Shaw RM. BIN1 localizes the L-type calcium channel to cardiac T-tubules. *PLoS Biol*. 2010;8:e1000312.

36. Hong TT, Smyth JW, Chu KY, Vogan JM, Fong TS, Jensen BC, Fang K, Halushka MK, Russell SD, Colecraft H, Hoopes CW, Ocorr K, Chi NC and Shaw RM. BIN1 is reduced and $Ca_V1.2$ trafficking is impaired in human failing cardiomyocytes. *Heart Rhythm*. 2012;9:812-20.

37. Lee E, Marcucci M, Daniell L, Pypaert M, Weisz OA, Ochoa GC, Farsad K, Wenk MR and De Camilli P. Amphiphysin 2 (Bin1) and T-tubule biogenesis in muscle. *Science*. 2002;297:1193-6.

38. Hong T, Yang H, Zhang SS, Cho HC, Kalashnikova M, Sun B, Zhang H, Bhargava A, Grabe M, Olgin J, Gorelik J, Marban E, Jan LY and Shaw RM. Cardiac BIN1 folds T-tubule membrane, controlling ion flux and limiting arrhythmia. *Nature medicine*. 2014;20:624-32.

39. Caldwell JL, Smith CER, Taylor RF, Kitmitto A, Eisner DA, Dibb KM and Trafford AW. Dependence of Cardiac Transverse Tubules on the BAR Domain Protein Amphiphysin II (BIN-1). *Circulation Research*. 2014;115:986-996.

40. De La Mata A, Tajada S, O'Dwyer S, Matsumoto C, Dixon RE, Hariharan N, Moreno CM and Santana LF. BIN1 Induces the Formation of T-Tubules and Adult-Like Ca^{2+} Release Units in Developing Cardiomyocytes. *Stem cells (Dayton, Ohio)*. 2019;37:54-64.

41. Pant S, Sharma M, Patel K, Caplan S, Carr CM and Grant BD. AMPH-1/Amphiphysin/Bin1 functions with RME-1/Ehd1 in endocytic recycling. *Nat Cell Biol*. 2009;11:1399-410.

42. Lambert E, Saha O, Soares Landeira B, Melo de Farias AR, Hermant X, Carrier A, Pelletier A, Gadaut J, Davoine L, et al. The Alzheimer susceptibility gene BIN1 induces isoform-dependent neurotoxicity through early endosome defects. *Acta Neuropathol Commun*. 2022;10:4.

43. Tan MS, Yu JT and Tan L. Bridging integrator 1 (BIN1): form, function, and Alzheimer's disease. *Trends in molecular medicine*. 2013;19:594-603.

44. Wang HF, Wan Y, Hao XK, Cao L, Zhu XC, Jiang T, Tan MS, Tan L, Zhang DQ, Tan L, et al. Bridging Integrator 1 (BIN1) Genotypes Mediate Alzheimer's Disease Risk by Altering Neuronal Degeneration. *J Alzheimers Dis*. 2016;52:179-90.

45. Chapuis J, Hansmannel F, Gistelinck M, Mounier A, Van Cauwenberghe C, Kolen KV, Geller F, Sottejeau Y, Harold D, Dourlen P, et al. Increased expression of BIN1 mediates Alzheimer genetic risk by modulating tau pathology. *Mol Psychiatry*. 2013;18:1225-34.

46. Cataldo AM, Peterhoff CM, Troncoso JC, Gomez-Isla T, Hyman BT and Nixon RA. Endocytic pathway abnormalities precede amyloid beta deposition in sporadic Alzheimer's disease and Down syndrome: differential effects of APOE genotype and presenilin mutations. *Am J Pathol*. 2000;157:277-86.

47. Schurmann B, Bermingham DP, Kopeikina KJ, Myczek K, Yoon S, Horan KE, Kelly CJ, Martin-de-Saavedra MD, Forrest MP, Fawcett-Patel JM, et al. A novel role for the late-onset Alzheimer's disease (LOAD)-associated protein Bin1 in regulating postsynaptic trafficking and glutamatergic signaling. *Mol Psychiatry*. 2020;25:2000-2016.

48. High KA and Aubourg P. rAAV Human Trial Experience. *Adeno-Associated Virus: Methods and Protocols*. 2011;807:429-457.

49. Josephson IR, Guia A, Stern MD and Lakatta EG. Alterations in properties of L-type Ca channels in aging rat heart. *J Mol Cell Cardiol*. 2002;34:297-308.

50. Dibb KM, Rueckschloss U, Eisner DA, Isenberg G and Trafford AW. Mechanisms underlying enhanced cardiac excitation contraction coupling observed in the senescent sheep myocardium. *J Mol Cell Cardiol*. 2004;37:1171-81.

51. Isenberg G, Borschke B and Rueckschloss U. Ca2+ transients of cardiomyocytes from senescent mice peak late and decay slowly. *Cell Calcium*. 2003;34:271-80.

52. Walker KE, Lakatta EG and Houser SR. Age associated changes in membrane currents in rat ventricular myocytes. *Cardiovascular research*. 1993;27:1968-77.

53. Liu SJ, Wyeth RP, Melchert RB and Kennedy RH. Aging-associated changes in whole cell K(+) and L-type Ca(2+) currents in rat ventricular myocytes. *Am J Physiol Heart Circ Physiol*. 2000;279:H889-900.

54. Kong CHT, Bryant SM, Watson JJ, Gadeberg HC, Roth DM, Patel HH, Cannell MB, Orchard CH and James AF. The Effects of Aging on the Regulation of T-Tubular ICa by Caveolin in Mouse Ventricular Myocytes. *J Gerontol A Biol Sci Med Sci*. 2018;73:711-719.

55. Esler MD, Thompson JM, Kaye DM, Turner AG, Jennings GL, Cox HS, Lambert GW and Seals DR. Effects of aging on the responsiveness of the human cardiac sympathetic nerves to stressors. *Circulation*. 1995;91:351-8.

56. Murphy E, Kohr M, Sun J, Nguyen T and Steenbergen C. S-nitrosylation: a radical way to protect the heart. *J Mol Cell Cardiol*. 2012;52:568-77.

57. Rueckschloss U, Villmow M and Klockner U. NADPH oxidase-derived superoxide impairs calcium transients and contraction in aged murine ventricular myocytes. *Exp Gerontol*. 2010;45:788-96.

58. Francis Stuart SD, Wang L, Woodard WR, Ng GA, Habecker BA and Ripplinger CM. Age-related changes in cardiac electrophysiology and calcium handling in response to sympathetic nerve stimulation. *J Physiol*. 2018;596:3977-3991.

59. Janczewski AM, Spurgeon HA and Lakatta EG. Action potential prolongation in cardiac myocytes of old rats is an adaptation to sustain youthful intracellular Ca2+ regulation. *J Mol Cell Cardiol*. 2002;34:641-8.

60. MacQuaide N, Tuan HT, Hotta J, Sempels W, Lenaerts I, Holemans P, Hofkens J, Jafri MS, Willems R and Sipido KR. Ryanodine receptor cluster fragmentation and redistribution in persistent atrial fibrillation enhance calcium release. *Cardiovascular research*. 2015;108:387-98.

61. Kolstad TR, van den Brink J, MacQuaide N, Lunde PK, Frisk M, Aronsen JM, Norden ES, Cataliotti A, Sjaastad I, Sejersted OM, Edwards AG, Lines GT and Louch WE. Ryanodine receptor dispersion disrupts Ca(2+) release in failing cardiac myocytes. *Elife*. 2018;7.

62. Hou Y, Bai J, Shen X, de Langen O, Li A, Lal S, Dos Remedios CG, Baddeley D, Ruygrok PN, Soeller C and Crossman DJ. Nanoscale Organisation of Ryanodine Receptors and Junctophilin-2 in the Failing Human Heart. *Front Physiol*. 2021;12:724372.

63. Dixon RE, Yuan C, Cheng EP, Navedo MF and Santana LF. Ca2+ signaling amplification by oligomerization of L-type Cav1.2 channels. *Proc Natl Acad Sci U S A*. 2012;109:1749-54.

64. Kettlewell S, Most P, Currie S, Koch WJ and Smith GL. S100A1 increases the gain of excitation-contraction coupling in isolated rabbit ventricular cardiomyocytes. *J Mol Cell Cardiol*. 2005;39:900-10.

65. Ubelmann F, Burrinha T, Salavessa L, Gomes R, Ferreira C, Moreno N and Guimas Almeida C. Bin1 and CD2AP polarise the endocytic generation of beta-amyloid. *EMBO Rep*. 2017;18:102-122.

66. Naslavsky N and Caplan S. EHD proteins: key conductors of endocytic transport. *Trends Cell Biol*. 2011;21:122-31.

67. Taga M, Petyuk VA, White C, Marsh G, Ma Y, Klein HU, Connor SM, Kroshilina A, Yung CJ, Khairallah A, et al. BIN1 protein isoforms are differentially expressed in astrocytes, neurons, and microglia: neuronal and astrocyte BIN1 are implicated in tau pathology. *Mol Neurodegener*. 2020;15:44.

68. Seals DR and Esler MD. Human ageing and the sympathoadrenal system. *J Physiol*. 2000;528:407-17.

69. Tang T, Hammond HK, Firth A, Yang Y, Gao MH, Yuan JX and Lai NC. Adenylyl cyclase 6 improves calcium uptake and left ventricular function in aged hearts. *Journal of the American College of Cardiology*. 2011;57:1846-55.

70. Narayanan N and Tucker L. Autonomic interactions in the aging heart: age-associated decrease in muscarinic cholinergic receptor mediated inhibition of beta-adrenergic activation of adenylate cyclase. *Mech Ageing Dev*. 1986;34:249-59.

71. Farrell SR and Howlett SE. The age-related decrease in catecholamine sensitivity is mediated by beta(1)-adrenergic receptors linked to a decrease in adenylate cyclase activity in ventricular myocytes from male Fischer 344 rats. *Mech Ageing Dev*. 2008;129:735-44.

Figures and Legends

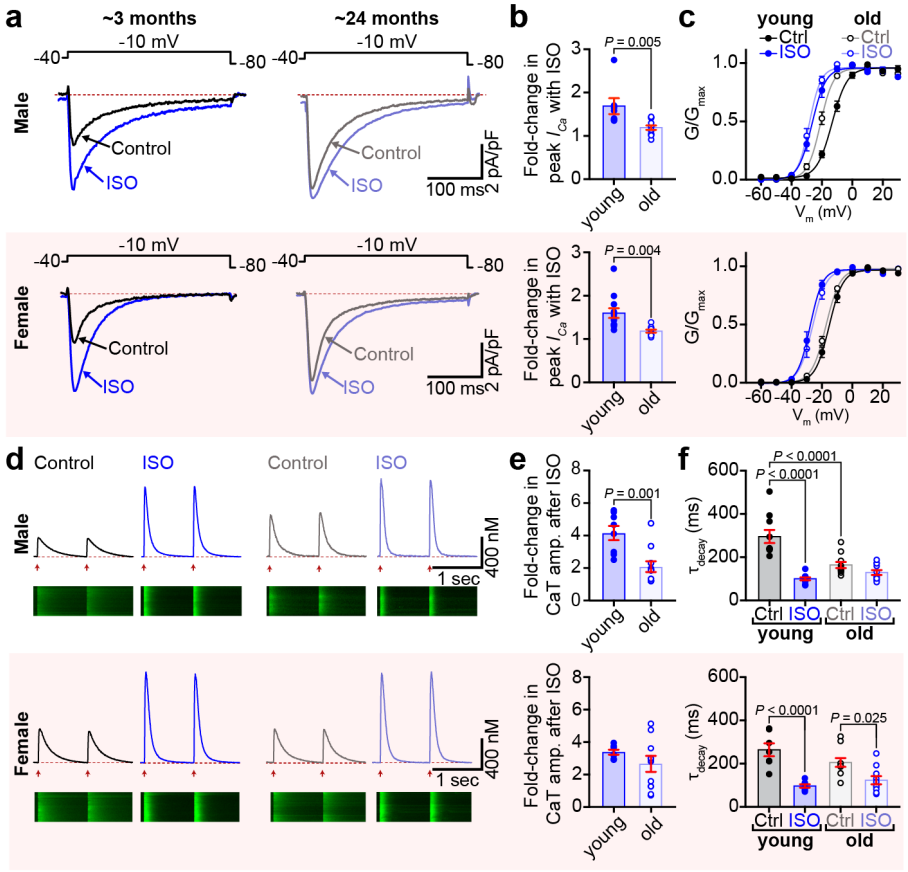

Figure 1. Functional analysis of *β*-AR stimulated augmentation of I_{Ca} and Ca^{2+} transients is diminished in aging. a, representative whole-cell currents elicited from young and old ventricular myocytes before (control; black) and during application of ISO (blue). **b**, dot-plots showing the fold change in peak current with ISO in male (young: *N* = 6, *n* = 7; old: *N* = 5, *n* = 12), and female (young: *N* = 5, *n* = 12; old: *N* = 5, *n* = 10) myocytes. **c**, voltage-dependence of the normalized conductance (G/G_{max}) fit with Boltzmann functions. **d**, representative Ca^{2+} transients recorded before and after ISO from paced male (young: *N* = 3, *n* = 8; old: *N* = 5, *n* = 11), and female (young: *N* = 3, *n* = 7; old: *N* = 3, *n* = 10) myocytes. **e**, dot-plots showing the fold-increase in Ca^{2+} transient (CaT) amplitude after ISO and **f**, Ca^{2+} transient τ_{decay} calculated from single exponential fits. Unpaired Student's t-tests were performed on data sets displayed in b and e. Two-way ANOVAs with post-hoc Tukey's multiple comparison tests were performed on data displayed in f.

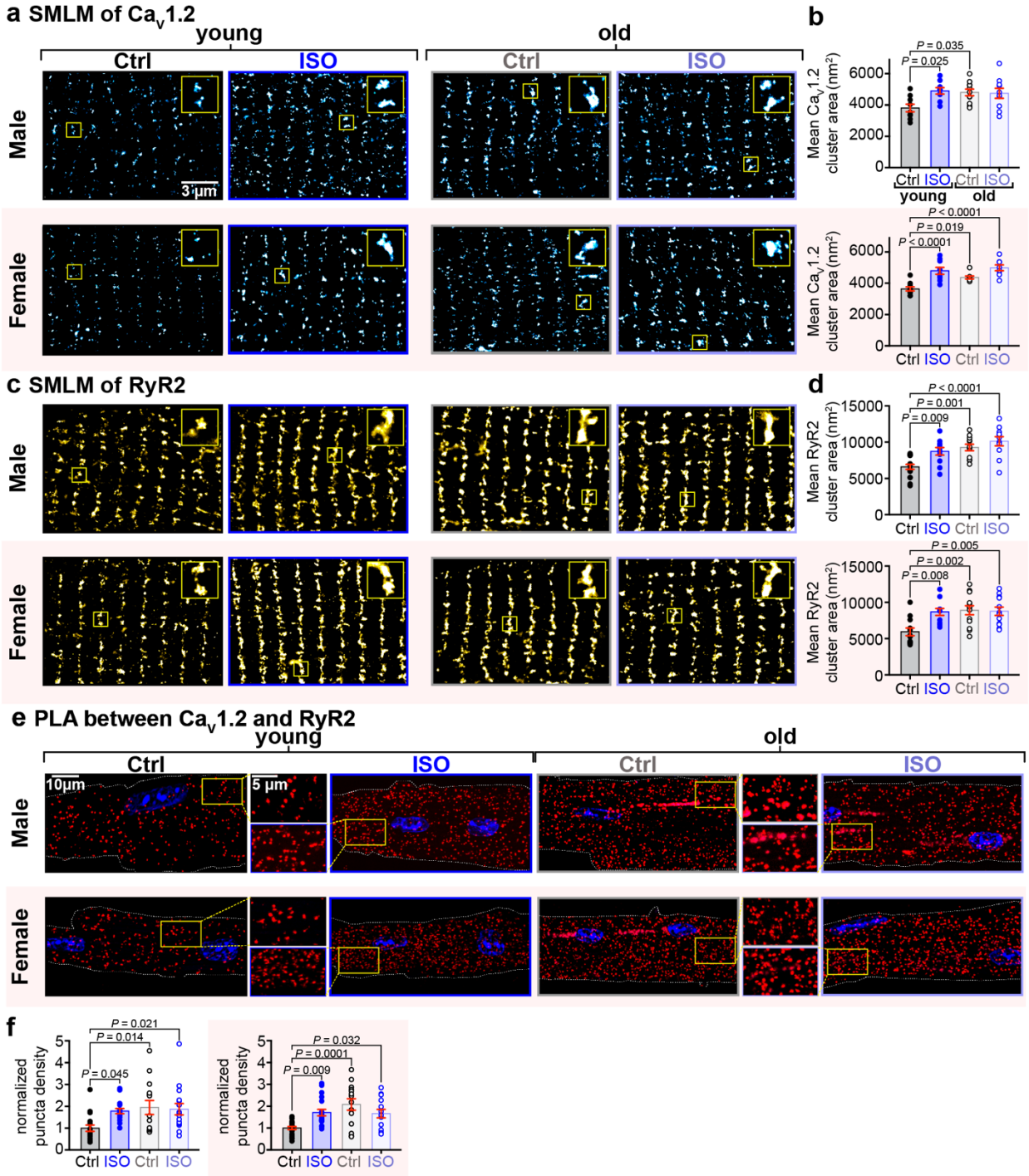

Figure 2. Basal super-clustering, impaired ISO-responsivity, and enhanced proximity of $Ca_V1.2$ and RyR2 in aged myocytes. **a**, SMLM localization maps showing $Ca_V1.2$ channel localization and distribution in the t-tubules of young and old ventricular myocytes with or without ISO-stimulation. Yellow boxes indicate the location of the regions of interest magnified in the top

right of each image. **b**, dot-plots showing mean $Ca_V1.2$ channel cluster areas in males (young control: *N* = 4, *n* = 9; young ISO: *N* = 3, *n* = 9; old control: *N* = 4, *n* = 11; old ISO: *N* = 4, *n* = 10) and females (young control: *N* = 3, *n* = 10; young ISO: *N* = 4, *n* = 9; old control: *N* = 3, *n* = 9; old ISO: *N* = 3, *n* = 8). **c** and **d**, show the same for RyR2 in males (young control: *N* = 3, *n* = 17; young ISO: *N* = 3, *n* = 11; old control: *N* = 3, *n* = 12; old ISO: *N* = 3, *n* = 11) and females (young control: *N* = 3, *n* = 12; young ISO: *N* = 3, *n* = 11; old control: *N* = 3, *n* = 13; old ISO: *N* = 3, *n* = 12). **e**, Representative fluorescence PLA (red)/DAPI (blue) images of male and female myocytes with and without ISO-stimulation. **f**, dot-plot summarizing the cellular density of PLA fluorescent puncta normalized to the density in young control cells from males (young control: *N* = 3, *n* = 19; young ISO: *N* = 3, = 16; old control: *N* = 3, *n* = 14; old ISO: *N* = 3, *n* = 16) and females (young control: *N* = 3, *n* = 20; young ISO: *N* = 3, *n* = 19; old control: *N* = 3, *n* = 14; old ISO: *N* = 3, *n* = 14). Statistical analyses on data summarized in b, d, and f were performed using two-way ANOVAs with post-hoc Tukey's multiple comparison tests.

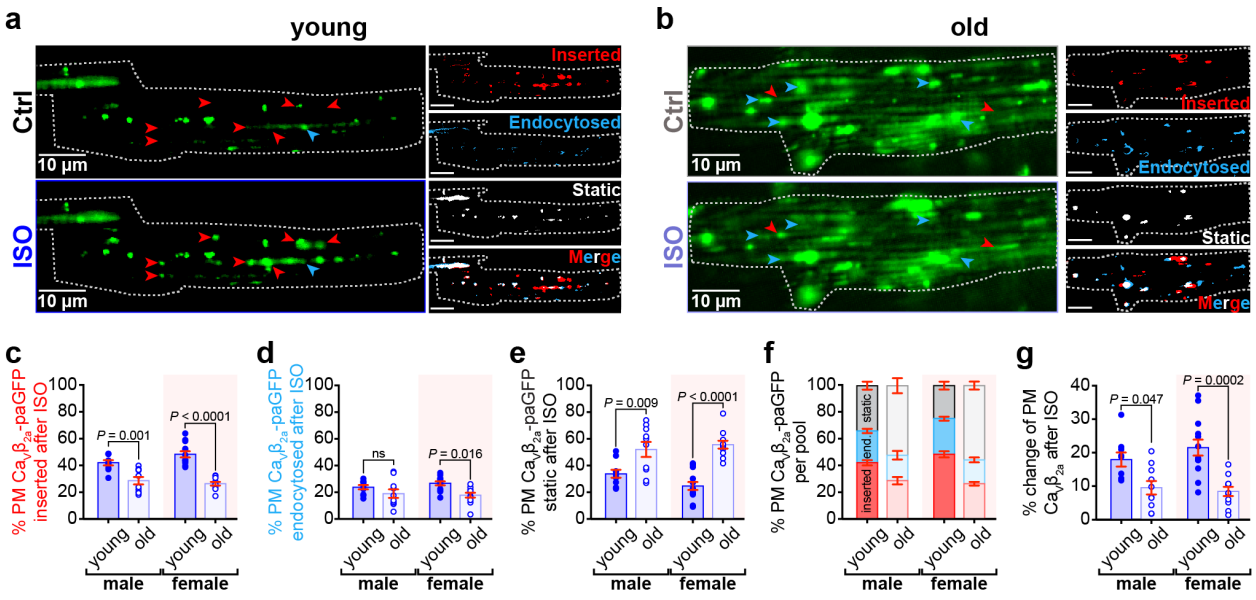

Figure 3. Dynamic TIRF imaging reveals age-associated trafficking deficits of $Ca_V1.2$.

a and **b**, Representative TIRF images of transduced $Ca_v\beta_{2a}$-paGFP young (**a**) and old (**b**) ventricular myocytes before (*top*) and after ISO (*bottom*). Channel populations that were inserted (red), endocytosed (blue), or static (white) during the ISO treatment are represented to the *right*. **c-e**, dot-plots summarizing the quantification of inserted (**c**), endocytosed (**d**), and static (**e**) $Ca_v\beta_{2a}$-paGFP populations. **f**, is a compilation of the data in c, d, and e to show the relative % of the channel pool that is inserted, endocytosed, and static. **g**, is a summary plot showing the net % change of plasma membrane $Ca_v\beta_{2a}$-paGFP after ISO for each cohort of male (young: $N = 3$, $n = 10$ and old: $N = 3$, $n = 10$) and female (young: $N = 3$, $n = 13$ and old: $N = 4$, $n = 11$) myocytes. Data were analyzed for statistical analysis using one-way ANOVAs with post-hoc Tukey's multiple comparison tests.

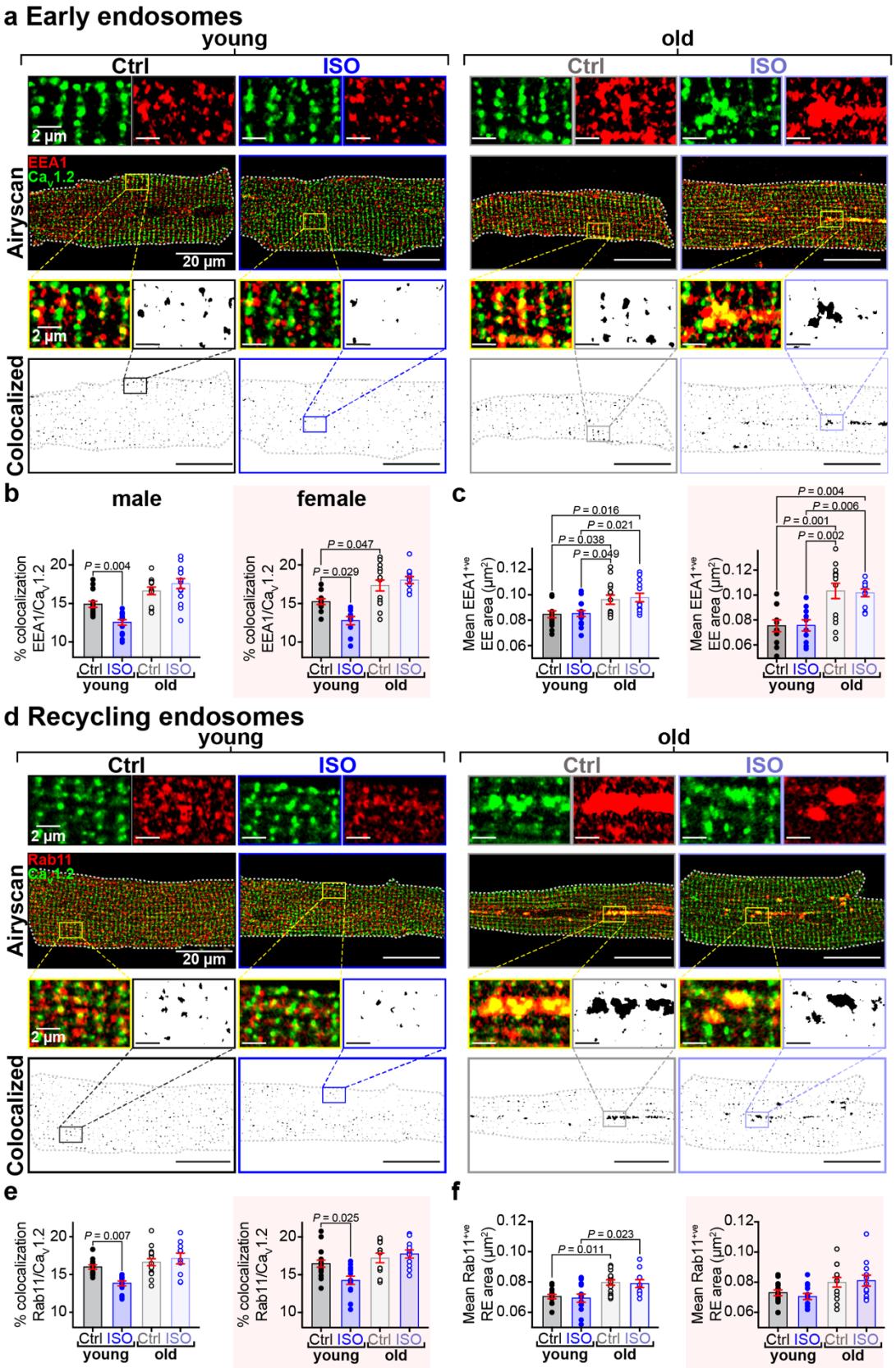
a Early endosomes
young
old
Ctrl
ISO
Airyscan
EEA1
Cav1.2
20 µm
2 µm
Colocalized
b
male
female
% colocalization EEA1/Cav1.2
P = 0.004
P = 0.029
P = 0.047
c
Mean EEA1+ve EE area (µm2)
P = 0.016
P = 0.021
P = 0.038
P = 0.049
P = 0.004
P = 0.006
P = 0.001
P = 0.002
d Recycling endosomes
Rab11
e
% colocalization Rab11/Cav1.2
P = 0.007
P = 0.025
f
Mean Rab11+ve RE area (µm2)
P = 0.011
P = 0.023

Figure 4. Aging impairs *β*-AR-stimulated Ca_v1.2 recycling. a, Airyscan super-resolution images of Ca_V1.2 and EEA1 immuno-stained myocytes with and without ISO. *Bottom:* Binary colocalization maps show pixels in which Ca_V1.2 and EEA1 completely overlapped. **b**, dot-plots summarizing % colocalization between EEA1 and Ca_V1.2, and **c**, EEA1 positive endosome areas in male (young control: *N* = 3, *n* = 16; young ISO: *N* = 3, *n* = 16; old control: *N* = 3, *n* = 14; old ISO: *N* = 3, *n* = 14) and female (young control: *N* = 3, *n* = 11; young ISO: *N* = 3, *n* = 10; old control: N = 3, n = 14; old ISO: *N* = 3, *n* = 11) myocytes. **d-f,** same layout for myocytes co-stained for Ca_V1.2 and Rab11 recycling endosomes in male (young control: *N* = 3, *n* = 13; young ISO: *N* = 3, *n* = 13; old control: *N* = 4, *n* =16; old ISO: *N* = 3, *n* = 10) and female (young control: *N* = 3, *n* = 16; young ISO: *N* = 3, *n* = 13; old control: *N* = 3, *n* = 13; old ISO: *N* = 3, *n* = 11) myocytes. Data were analyzed using two-way ANOVAs with post-hoc Tukey's multiple comparison tests.

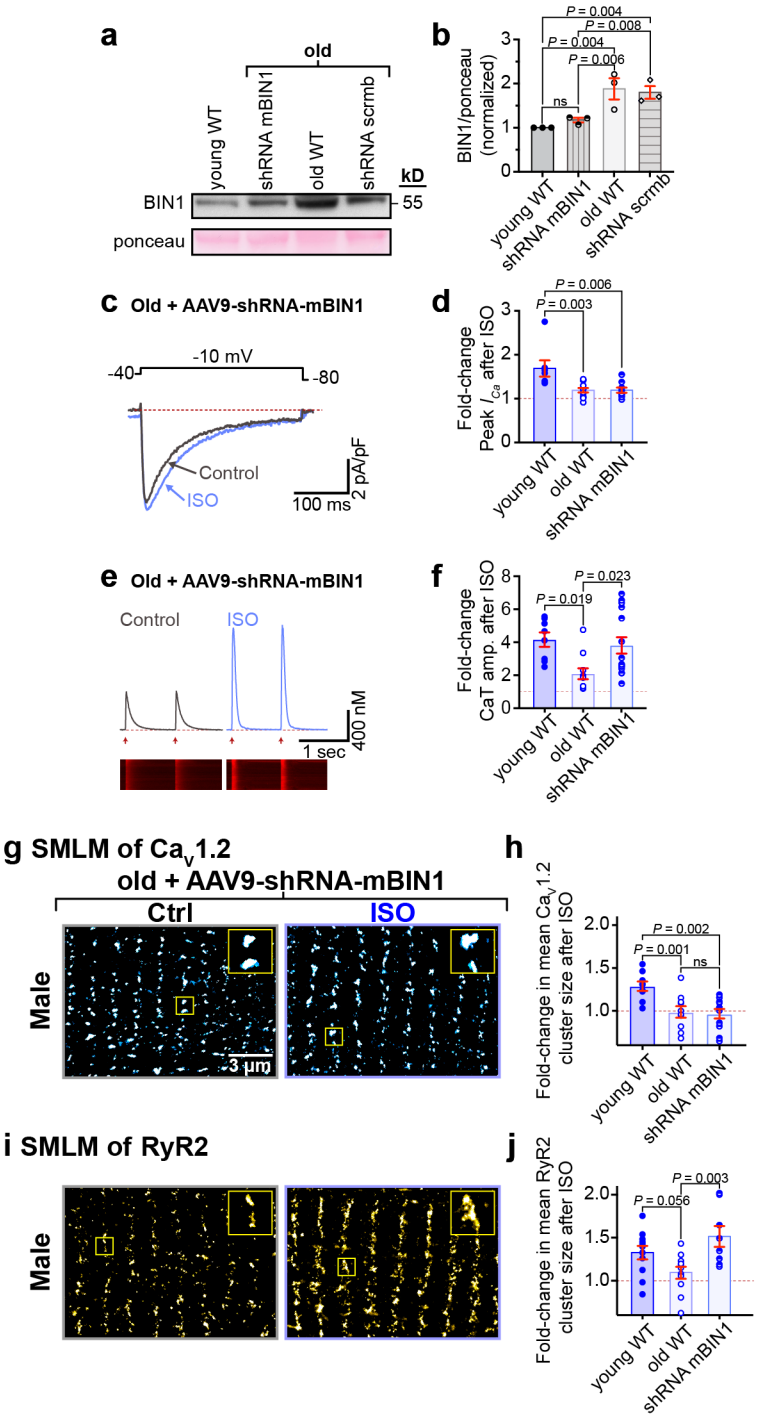

Figure 5. BIN1 knockdown restores β-AR augmentation of Ca^{2+} transients and RyR2 clustering dynamics. a, western analysis of BIN1 protein expression in whole heart lysates from male mice from the following groups: young, old, old transduced with shRNA-mBIN1, or old transduced with shRNAscrmb (all N = 3, n = 3). Ponceau shows total protein which was used for

normalization. **b**, summary histogram showing normalized BIN1 levels in each group relative to young control. **c**, representative whole-cell currents from shRNA-BIN1 transduced old male myocytes before and during application of ISO. **d**, summary histogram comparing the fold change in peak I_{Ca} with ISO in young, old, and shRNA-mBIN1 transduced old myocytes (N = 3, n = 9). Old and young data points are reproduced from Figure 1b. **e**, representative Ca^{2+} transients recorded from old male shRNA-mBIN1 transduced myocytes before and after ISO. **f**, summary histogram of the fold increase after ISO from young (N = 3, n = 8), old (N = 5, n = 11), and shRNA-mBIN1 transduced old male mice (N = 5, n = 14). Old and young data points are reproduced from Figure 1e. **g**, SMLM localization maps showing $Ca_V1.2$ channel localization on the t-tubules of myocytes isolated from old male shRNA-BIN1 transduced mice, with or without ISO-stimulation. Yellow boxes indicate the location of the regions of interest magnified in the top right of each image. **h**, dot-plots showing the fold change in mean $Ca_V1.2$ channel cluster area after ISO in the old shRNA-mBIN1 cells (control: N = 3, n = 12; ISO: N = 3, n = 11). The fold change in mean $Ca_V1.2$ channel cluster area after ISO in young WT myocytes previously highlighted in Figure 2a and 2b is shown for comparison. **i** and **j**, show the same layout for RyR2 immunostained old shRNA-mBIN1 myocytes (control: N = 3, n = 9; ISO: N = 3, n = 8) with the summary showing comparison to the dataset previously shown in Figure 2c and d. Statistical analyses were performed using one-way ANOVAs.